Check for updates

Received: 16 April 2023 | Accepted: 13 May 2023

DOI: 10.1111/1462-2920.16430

RESEARCH ARTICLE

ENVIRONMENTAL MICROBIOLOGY Applied Microbiology International

Life strategies and metabolic interactions of core microbes during thiosulphate-based denitrification

Shengjie Li[1,2] | **Yinhao Liao**[1] | **Zhuo Jiang**[1] | **Guodong Ji**[1]

[1]Key Laboratory of Water and Sediment Sciences, Ministry of Education, Department of Environmental Engineering, Peking University, Beijing, China

[2]Department of Biogeochemistry, Max Planck Institute for Marine Microbiology, Bremen, Germany

Correspondence
Guodong Ji, Key Laboratory of Water and Sediment Sciences, Ministry of Education, Department of Environmental Engineering, Peking University, Beijing 100871, China.
Email: jiguodong@pku.edu.cn

Funding information
Foundation for Innovative Research Groups of the National Natural Science Foundation of China, Grant/Award Number: 51721006; National Key Research and Development Project of China, Grant/Award Number: 2019YFC0409200; High-performance Computing Platform of Peking University

Abstract

Sulphur-driven denitrification is a low-cost process for the treatment of nitrate-contaminated water. However, a comprehensive understanding of core populations and microbial interactions of a sulphur-based denitrifying system is lacking. This study presents results from three replicated denitrifying systems amended with thiosulphate and operated under a low C/N ratio. Amplicon sequencing revealed gradual enrichments of a few abundant denitrifiers. Based on genome-centred metagenomics and metatranscriptomics, a core set of microbes was identified in the systems, with *Pseudomonas* 1 and *Thauera* 2 being the most abundant ones. Although the replicates showed different enrichments, generalized observations were summarized. Most core populations conserved energy from denitrification coupled with sulphur. *Pseudomonas* 1 and *Thauera* 2 were able to finish complete denitrification. Surprisingly, they were also able to synthesize almost all amino acids and vitamins. In contrast, less abundant members, including *Pseudomonas* 2, were relatively auxotrophic and required an exogenous supply of amino acids and vitamins. The high expression of enzymes involved in biosynthesis and transport systems indicated their syntrophic relationships. The genomic findings suggested life strategies and interactions of the core thiosulphate-based denitrifying microbiome, with implications for nitrate-polluted water remediation.

INTRODUCTION

Due to the increased use of fertilizer, large quantities of nitrogen are entering water bodies, including rivers and lakes (Mekonnen & Hoekstra, 2015). This leads to great eutrophication problems in aquatic environments. Denitrification undertakes the greatest part of nitrogen removal in nature (Seitzinger, 2008). Diverse forms of organic compounds are favourable electron donors for microbial denitrification. However, surface water is typical of low organic carbon content compared to nitrate (Newcomer et al., 2012), demonstrating a lack of electron donors compared to electron acceptors for heterotrophic denitrifiers. Sulphur-dependent autotrophic denitrification uses inorganic carbon as the carbon source and reduced forms of sulphur as the energy source. As a low-cost technique, it receives increasing attention for the remediation of nitrate-contaminated water (Della Rocca et al., 2007; Li et al., 2016, 2017).

Previous work elucidated that *Thiobacillus* and *Sulfurimonas* were the commonly observed species in autotrophic sulphur-driven denitrifying bioreactors (Shao et al., 2010). However, in aquatic ecosystems with the presence of both nitrogen and organic pollutants, two situations might happen after sulphur amendment. The first is the enrichment of a core microbiome, which simultaneously uses organic and inorganic electron donors to reduce nitrate. The other is the abundance of two microbial groups with distinct functions—one group conducts heterotrophic denitrification and the other group conducts autotrophic denitrification. Based on 16S rRNA amplicon sequencing, some studies suggested autotrophic and heterotrophic denitrifiers jointly contributed to nitrogen removal in sulphur-driven denitrifying systems with organic supplementation (Han

© 2023 Applied Microbiology International and John Wiley & Sons Ltd.

et al., 2020; Qiu et al., 2020; Zhang et al., 2015; Zhang et al., 2018), which indicated the possibility of the second situation. Metagenomic analysis revealed a high abundance of genes involved in nitrogen, sulphur, and carbon metabolisms during autotrophic-heterotrophic denitrification (Zhang et al., 2020). However, genome characteristics and transcriptional activity of main microorganisms have not been studied. Function viability and life strategies of core populations in sulphur-dependent denitrifying consortia were not well reported, but this is important to understand nitrate removal performance.

Interactions among populations formed the basis of the microbial world and significantly shaped community assembly and succession processes (Faust & Raes, 2012). The other unresolved problem for sulphur-based denitrifying systems is how functional microbes interact with each other in the community. Microbes are likely to cooperate to finish denitrification. Evidence is growing that few organisms conduct complete denitrification, with most denitrifiers able to reduce only one or a few nitrogen oxides (Kuypers et al., 2018). For example, some organisms may lack reductases for nitrate and others may lack reductases for nitric oxide (NO) and nitrous oxide (N_2O), which was the scenario in some reported nitrate-reducing consortia (Haroon et al., 2013; He et al., 2016; Li, Jiang, & Ji, 2022). Currently, we do not know what exact role each functional microbe plays in sulphur-based denitrification.

In addition, microorganisms may lose enzymes for biosynthesis of growth-required substances (e.g., am ino acids, vitamins, and cofactors) during evolution to reduce metabolic burden. Instead, they rely on other community members to obtain these substances. The reduction of genomic content and dependence between community members are presented as the Black Queen Hypothesis (Morris et al., 2012), which indicates "beneficiaries" (auxotrophs) with gene loss depend on "helpers" (prototrophs). Such dependence may happen to a considerable extent and regulate nitrogen removal. A comprehensive understanding of microbial interactions will therefore provide new insights into this process, but the syntrophic relationship has not been studied in a sulphur-based denitrifying system.

The current study aimed to investigate microbial structures, life strategies, and interactions among populations during sulphur-dependent denitrification. According to previous research, thiosulphate was the most efficient electron donor for sulphur-dependent microbial denitrification (Li, Jiang, & Ji, 2022; Zhou et al., 2016). We established denitrifying systems with and without thiosulphate amendment and operated the systems at a low C/N ratio. Amplicon sequencing examined the community assembly process. Genome-centric metagenomic analysis revealed the functional potentials of a core set of microbes. Particularly, aligning RNA reads to single genomes allowed in-depth analysis of the transcriptional activity of core populations. The integrated approaches improved our understanding of the microbial world underlying sulphur-driven denitrification and shed light on modulating nitrogen removal performance during ecological remediation.

EXPERIMENTAL PROCEDURES

Experimental setup and operation

Denitrifying microbial consortia were enriched from water and sediment samples collected from the Guangfu River, China. The basic medium contained 2.0 mM $MgCl_2 \cdot 6H_2O$, 0.90 mM $CaCl_2$, 11 mM KH_2PO_4, 0.5 mM NH_4Cl, 10 mM $NaHCO_3$, 1.0 mL trace element solution, and 1.0 mL vitamin solution (Li, Mosier, et al., 2022). The trace element solution contained (per litre) $FeSO_4 \cdot 7H_2O$ (1 g), $ZnCl_2$ (0.07 g), $MnCl_2 \cdot 2H_2O$ (0.1 g), H_3BO_3 (0.03 g), $CoCl_2 \cdot 6H_2O$ (0.02 g), $CuSO_4 \cdot 5H_2O$ (0.02 g), $NiCl_2 \cdot 6H_2O$ (0.02 g) and $Na_2MoO_4 \cdot 2H_2O$ (0.04 g). There were two treatments, (a) adding nitrate and acetate, (b) adding nitrate, acetate, and thiosulphate. Triplicated systems were set up for each treatment. Twenty gramme water-sediment samples were inoculated into each replicate with a total volume of 0.4 L. The systems ran for six phases in the dark in a shaker (100 rpm). For (a), each phase ended when total organic carbon (TOC) was almost consumed and there was almost no nitrate reduction activity. For (b), each phase ended when nitrate was fully reduced. At the end of each phase, 0.2 L culture was replaced with 0.2 L fresh basic medium. At the start of each phase, 6.0 mM $NaNO_3$ and 1.5 mM CH_3COONa were added to (a), while 6.0 mM $NaNO_3$, 1.5 mM CH_3COONa and 4.0 mM $Na_2S_2O_3$ were added to (b). The systems were flushed with nitrogen to create anoxic environments. Rubber stoppers and aluminium crimp caps were used to seal the systems during operation and sampling.

Sampling and wet chemistry analysis

For each time of sampling, 5 mL samples were collected from the systems with syringes after homogenizing. The samples were centrifuged at 5000 rpm for 10 min. The pellets were used for DNA and RNA extraction. The supernatants were filtered with 0.2 μm membranes. For filtrate, nitrate, and sulphate concentrations were measured with an ion chromatograph (Li et al., 2021). TOC content was measured with a TOC analyser (TOC-L CPH, Shimadzu, Japan). Ammonia was measured using the indophenol reaction with a

14622920, 2023, 10, Downloaded from https://ami-journals.onlinelibrary.wiley.com/doi/10.1111/1462-2920.16430 by MPI 317 Marine Microbiology, Wiley Online Library on [22/01/2024]. See the Terms and Conditions (https://onlinelibrary.wiley.com/terms-and-conditions) on Wiley Online Library for rules of use; OA articles are governed by the applicable Creative Commons License

spectrophotometer at 625 nm (Shimadzu, Japan) (McCullough, 1967).

DNA extraction and amplicon sequencing

DNA samples were collected at the start of the system running and at the end of each phase. DNA was extracted with the FastDNA Spin Kit for Soil (MP Biomedicals, USA) and checked for quality with 1% agarose gel electrophoresis. Primers 338F and 806R were used to amplify the 16S rRNA gene (Li et al., 2018). PCR systems were prepared and PCR reactions were conducted according to previously described methods (Li, Jiang, & Ji, 2022). Amplicons were subjected to paired-end sequencing on the Illumina MiSeq sequencing platform using PE300 chemical at Majorbio Bio-Pharm Technology Co. Ltd. (Shanghai, China).

After demultiplexing, the resulting sequences were merged with FLASH v1.2.11(Magoc & Salzberg, 2011) and quality-filtered with fastp v0.19.6 (Chen et al., 2018). Quality-controlled sequences were denoised using the DADA2 plugin in QIIME 2 v2020.2 (Callahan et al., 2016). Non-metric multidimensional scaling (NMDS) was performed with 'dplyr' and 'vegan' packages in R v4.0.5.

Metagenomic sequencing and analysis

Six metagenomic samples were collected from each system at the end of the operation (2 treatments $\times$ 3 replicates $=$ 6 samples). Sequencing was conducted according to a previously described method (Li, Liao, et al., 2022). Briefly, DNA was fragmented to about 400 bp, ligated to adapters, and sequenced with Illumina NovaSeq 6000 platform using NovaSeq Reagent Kits.

Quality control of the raw reads was performed with BBDuk. The filtered reads were assembled using MEGAHIT v1.2.9 (Li et al., 2015). Only contigs longer than 500 bp were kept for further analysis. The reads were mapped to the assembled contigs with BBmap v38.18 using "minid $=$ 0.99". The sequencing depth for each contig in the six metagenomes was calculated with the "jgi_summarize_bam_contig_depths" script from MetaBat v2:2.15 (Kang et al., 2019). The contigs were binned into metagenome-assembled-genomes (MAGs) with MetaBat v2:2.15. The obtained MAGs from different libraries were dereplicated using dRep v3.2.2 (Olm et al., 2017). The quality of the MAGs was estimated with CheckM v1.1.3 (Parks et al., 2015). The MAGs were assigned taxonomically with GTDB-Tk v1.0.2 (Parks et al., 2018). The six libraries of contigs (binned and unbinned) were merged and redundant contigs were removed with cd-hit, where preference was given to binned contigs (Li & Godzik, 2006). The sequencing depth of the final non-redundant contigs was obtained using the same method for calculating the sequencing depth of the contigs in each library. The relative abundance of a MAG in the six samples was calculated by dividing the sequencing depth of the MAG by the sum of sequencing depths of all non-redundant contigs. The MAGs were annotated with Prokka v1.13(Seemann, 2014) and METABOLIC v4.0 (Zhou et al., 2022). Hidden Markov Models (HMMs) v3.3.2 (Eddy, 2008) were run for the detection of genes involved in denitrification according to a previous method (Li et al., 2021). The MAGs were blasted against the KEGG database to recognize genes for the biosynthesis of amino acids and vitamins. Transporters were annotated with TransAAP (http://www.membranetransport.org/transaap/TransAAP_login.html). For a comparison of gene abundance among the metagenomes, the sequencing depth of the gene was compared to the average sequencing depth of all genes for each metagenome.

The fast-format sequence file of the genome of *Pseudomonas* sp. C27 (Chen et al., 2013; Zhang et al., 2020) was downloaded from the GenBank database for comparison with the MAGs recovered in this study. The same approaches were used to annotate it as used for MAGs.

RNA extraction, metatranscriptomic sequencing, and analysis

Six metatranscriptomic samples were collected in accordance with the six metagenomic samples. Total RNAs were extracted using the E.Z.N.A.® Soil RNA Midi Kit (Omega Bio-tek, Norcross, GA, USA) according to the manufacturer's protocols. RNA concentrations were quantified with NanoDrop2000 (Thermo Fisher Scientific, U.S.). RNA quality was examined with the 1% agarose gel electrophoresis system and assessed using an RNA6000 Nano chip (total RNA) in an Agilent 2100 Bioanalyzer.

Total RNA was subjected to an rRNA removal procedure using the Ribo-zero Magnetic kit according to the manufacturer's instruction (Epicentre, an Illumina® company). cDNA libraries were constructed using TruSeq™ RNA sample prep kit (Illumina). The barcoded libraries were sequenced on the Illumina Hiseq 2500 platform using HiSeq 4000 PE Cluster Kit and HiSeq 4000 SBS Kits.

3′ and 5′ ends were stripped using SeqPrep (https://github.com/jstjohn/SeqPrep). Low-quality reads (length <50 bp or with a quality value <20 or having N bases) were removed by Sickle (https://github.com/najoshi/sickle). SortMeRNA v2.1b was applied to remove ribosomal RNA (Kopylova et al., 2012). The filtered reads were mapped to the

14622920, 2023, 10, Downloaded from https://ami-journals.onlinelibrary.wiley.com/doi/10.1111/1462-2920.16430 by MPI 317 Marine Microbiology, Wiley Online Library on [22/01/2024]. See the Terms and Conditions (https://onlinelibrary.wiley.com/terms-and-conditions) on Wiley Online Library for rules of use; OA articles are governed by the applicable Creative Commons License

non-redundant contigs using BBmap v38.18 with the same parameters as used for metagenomic reads. The sequencing depth of each contig and relative abundance of each MAG in the metatranscriptomes were calculated with the same methods as used in the metagenomic analysis.

For analysis of core microbes, a set of populations with a total relative abundance of more than 50% for both metagenome and metatranscriptome was identified. Genomes and transcriptomes of each population were individually analysed. HTSeq v1.99.2 was applied to obtain the sequencing depth of each gene in each MAG (Anders et al., 2015). Transcripts per million (TPM) of each gene were calculated based on the transcriptome of a single population, regardless of the influence of the relative abundance of the populations in metatranscriptomes. The expression of genes involved in the biosynthesis of amino acids and vitamins was calculated as the sum of the transcriptional abundance of all required genes for one substance.

RESULTS

Nitrate removal

In the systems with only acetate, the three replicates (named C1, C2, and C3) showed similar performances. About half of the nitrate remained at the end of each phase (Figure 1A). In the systems amended with thiosulphate, two replicates (named S1 and S2) fully reduced nitrate, while the other replicate (named S3) reduced nitrate during the first and the second phases (Figure 1B). Afterwards, the three replicates showed similar nitrate removal efficiency. Nitrite accumulated in the systems without thiosulphate but was consumed at the end of each phase in the thiosulphate-based systems (Figure S1a,b). For both treatments, acetate was highly utilized, while the systems with thiosulphate consumed slightly less acetate (about 0.3 mM) than the systems with only acetate during each phase (Figure 1C,D). In the systems with only acetate, sulphate concentrations were reduced by half during each transfer and finally under detection limitation at the sixth phase (Figure 1E). About 8 mM sulphate was produced from sulphur oxidation during each phase in the systems with thiosulphate (Figure 1F). This indicated thiosulphate acted as an efficient electron donor for denitrification when organic carbon was lacking compared to nitrate. Ammonia concentrations gradually decreased during each phase in both treatments (Figure S1c,d). There was no obvious ammonia production, indicating dissimilatory nitrate reduction to ammonia was less active and denitrification mainly accounted for the nitrate removal performance in the systems.

Microbial community assembly

The assembly of microbial communities was monitored with ASVs in each replicate of the two treatments (Figure 2). In the beginning, *Delftia* and *Variovorax* were the most abundant populations in amplicon libraries, indicating they were the main residents of the river (Figure 2A). After adding acetate, several populations affiliated with *Azoarcus*, *Bdellovibrio*, *Vogesella*, and *Thauera* gradually increased in relative abundance. At the end of the experiment, enriched genera included those affiliated with *Comamonadaceae* and *Rhodocyclaceae*. For the thiosulphate-based systems, community structure showed some variance among the replicates. In two of the replicated systems (S1 and S2), *Pseudomonas* a (about 40%) and *Thiobacillus* a (about 20%) were gradually enriched and became the most abundant members. In the other replicate (S3), the most abundant member was *Thauera* a with the final relative abundance of 27%. NMDS analysis showed that differences between the two treatments were more evident than variance among replicates (Figure 2B). Distinct community succession patterns from similar start points were observed for the two treatments, indicating microbial communities underwent obvious changes and different populations were enriched with and without thiosulphate.

Enriched populations recovered by metagenomes

Fifty-five MAGs, whose completeness was over 70% and contamination was less than 10%, were obtained in total. They included 25 MAGs affiliated with *Proteobacteria* and 11 MAGs affiliated with *Bacteroidota* (Table S1). Together, these populations accounted for more than 98% of the total quality-filtered DNA and mRNA reads (Figure 3, Table S2). In the systems without thiosulphate, the three replicates showed similar enrichments. A core set of microbes including 10 populations was identified (indicated with green stars in Figure 3). In total, they explained over 50% of the metagenomes and metatranscriptomes of the three replicated systems. All of the core populations contained at least one enzyme encoding genes involved in denitrification and could directly oxidize acetate.

In the systems with thiosulphate, the three replicates showed different enrichments, and different populations were included in core microbiomes (Figure 3). Generally, an organism with a relative abundance of more than 4% in any of the metagenomes was defined as a core population. Together, the core microbiome at least accounted for 55% of both metagenomes and metatranscriptomes. For S1, core populations included *Pseudomonas* 1 (22% in the

14622920, 2023, 10, Downloaded from https://ami-journals.onlinelibrary.wiley.com/doi/10.1111/1462-2920.16430 by MPI 317 Marine Microbiology, Wiley Online Library on [22/01/2024]. See the Terms and Conditions (https://onlinelibrary.wiley.com/terms-and-conditions) on Wiley Online Library for rules of use; OA articles are governed by the applicable Creative Commons License

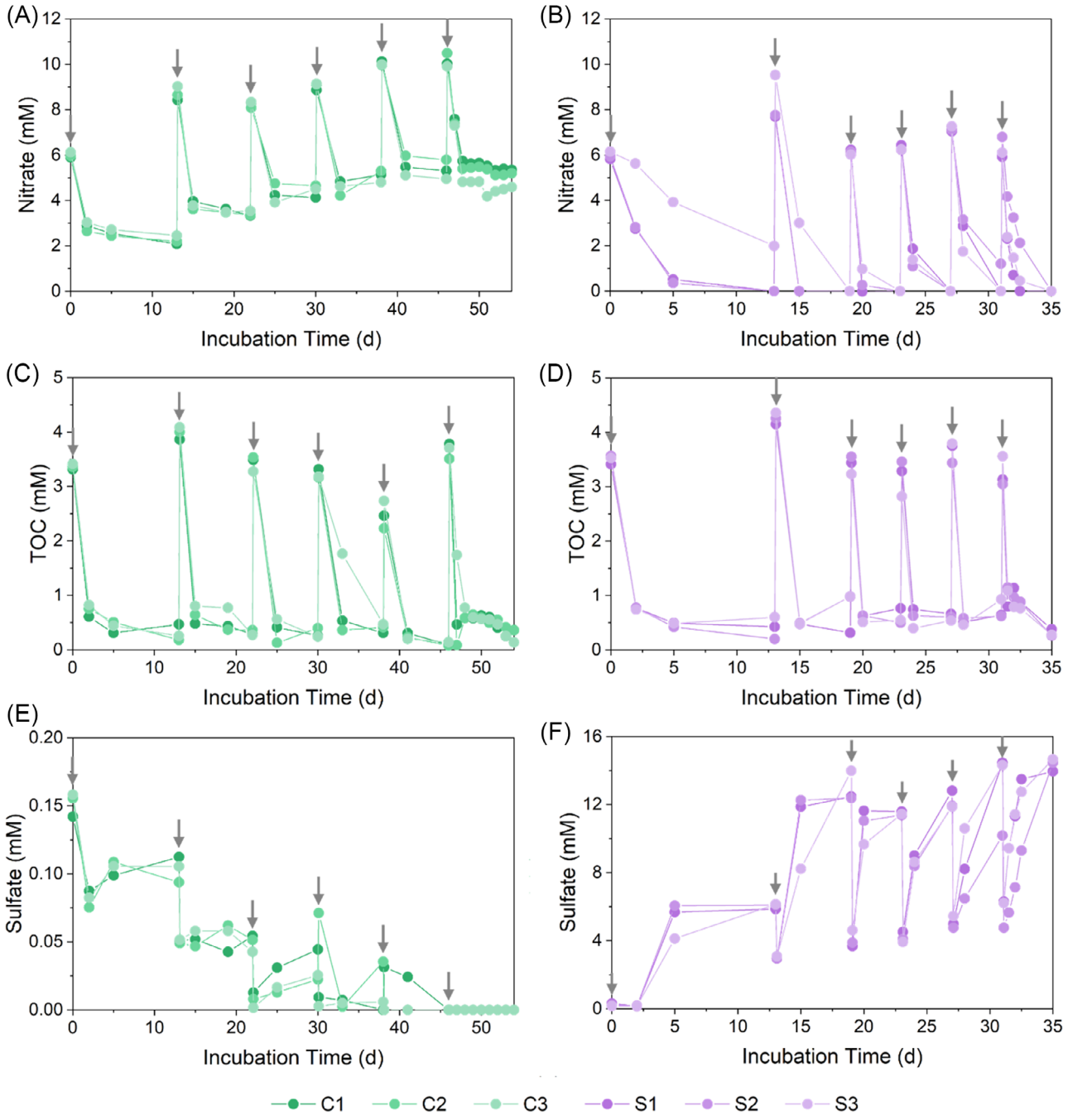

FIGURE 1 The concentration change of (A, B) nitrate, (C, D) total organic carbon (TOC), and (E, F) sulphate in (A, C, E) the systems with only acetate and (B, D, F) the systems with both acetate and thiosulphate. Down arrows indicate time points when nitrate, acetate, and thiosulphate were added. The systems were operated anoxically during the entire experiment. The three replicates of the systems with only acetate are named C1, C2, and C3. The three replicates of the systems with thiosulphate are named S1, S2, and S3.

metagenome), *Thiobacillus* 2 (14%), *Burkholderiaceae* 4 (11%), *Gracilibacteria* (9%), and *Thauera* 2 (4%). Surprisingly, *Gracilibacteria*, the population belonging to a candidate phylum, was enriched to 8% in S1. The discovered *Gracilibacteria* population did not encode any function related to carbon, nitrogen, and sulphur cycling pathways. In S2, core populations only included *Pseudomonas* 1 (72%) and *Bacteroidales* 1 (9%). In S3, core populations included *Thauera* 2 (53%), *Thiobacillus* 2 (5%), *Flavobacteriaceae* (4%), and *Flavobacterium* (4%). The most abundant populations *Pseudomonas* 1 (S1 and S2) and *Thauera* 2 (S3) were able to conduct complete denitrification, while other less abundant members may not contain some reductases. For example, *Bacteroidales* 1 could not reduce N_2O, *Flavobacteriaceae* could not reduce nitrite to NO

14622920, 2023, 10, Downloaded from https://ami-journals.onlinelibrary.wiley.com/doi/10.1111/1462-2920.16430 by MPI 317 Marine Microbiology, Wiley Online Library on [22/01/2024]. See the Terms and Conditions (https://onlinelibrary.wiley.com/terms-and-conditions) on Wiley Online Library for rules of use; OA articles are governed by the applicable Creative Commons License

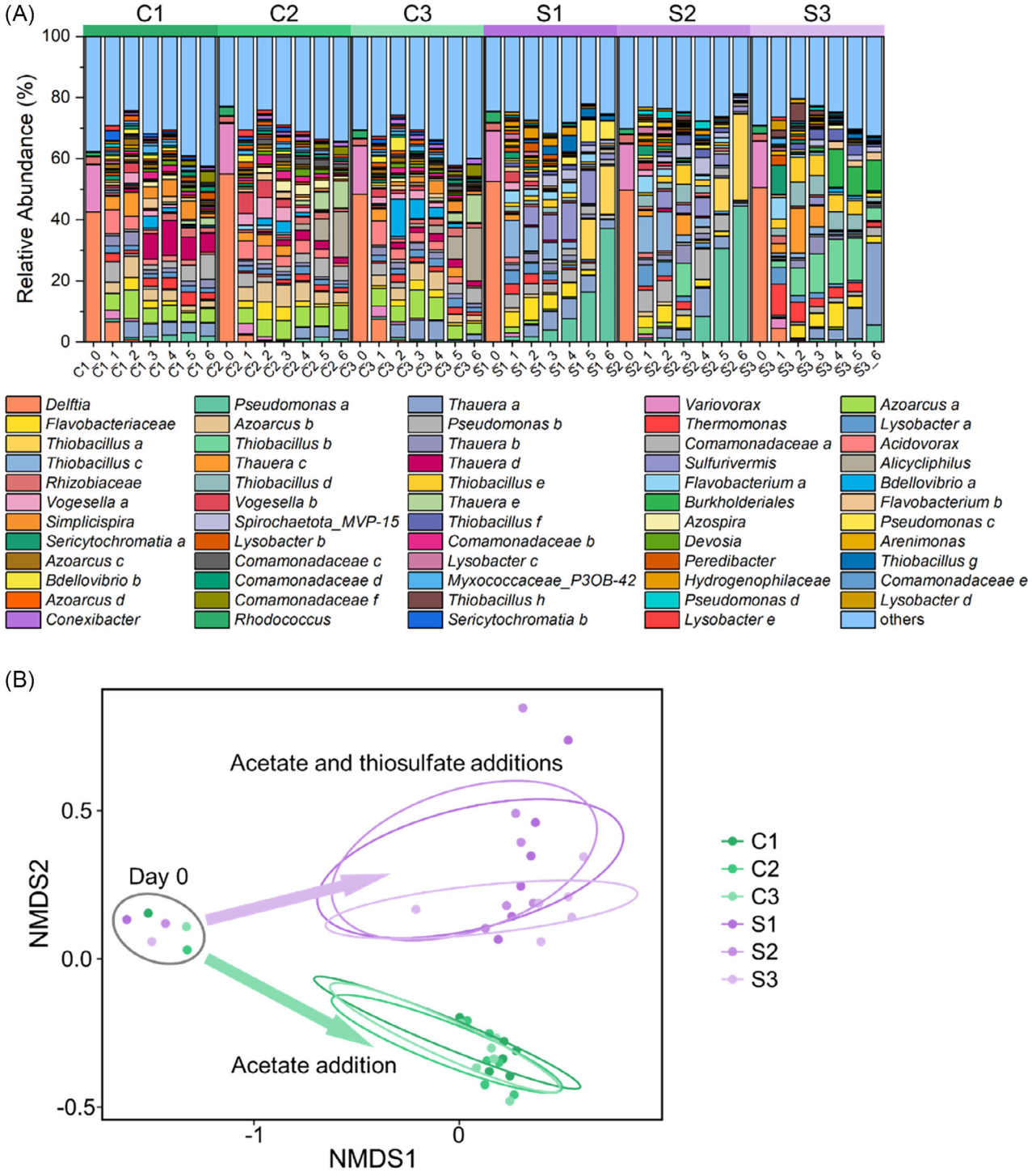

FIGURE 2 (A) Change in the relative abundance of microbes based on relative sequence abundance of amplicon sequencing variants (ASVs). (B) Microbial community assembly and succession revealed by non-metric multidimensional scaling (NMDS).

and *Flavobacterium* did not contain any nitrate reductase. Most of them (except *Gracilibacteria* and *Flavobacterium*) were able to use both sulphur and organic carbon as energy sources. Among all core populations, only the genome of *Thiobacillus* 2 contained enzyme-encoding genes involved in a carbon fixation pathway, the Calvin Cycle.

Expression of biochemical cycling pathways

The abundance of functional genes involved in key metabolic pathways was normalized by the average abundance of all genes in metagenomes or metatranscriptomes (Figure 4A). We did not observe the

14622920, 2023, 10, Downloaded from https://ami-journals.onlinelibrary.wiley.com/doi/10.1111/1462-2920.16430 by MPI 317 Marine Microbiology, Wiley Online Library on [22/01/2024]. See the Terms and Conditions (https://onlinelibrary.wiley.com/terms-and-conditions) on Wiley Online Library for rules of use; OA articles are governed by the applicable Creative Commons License

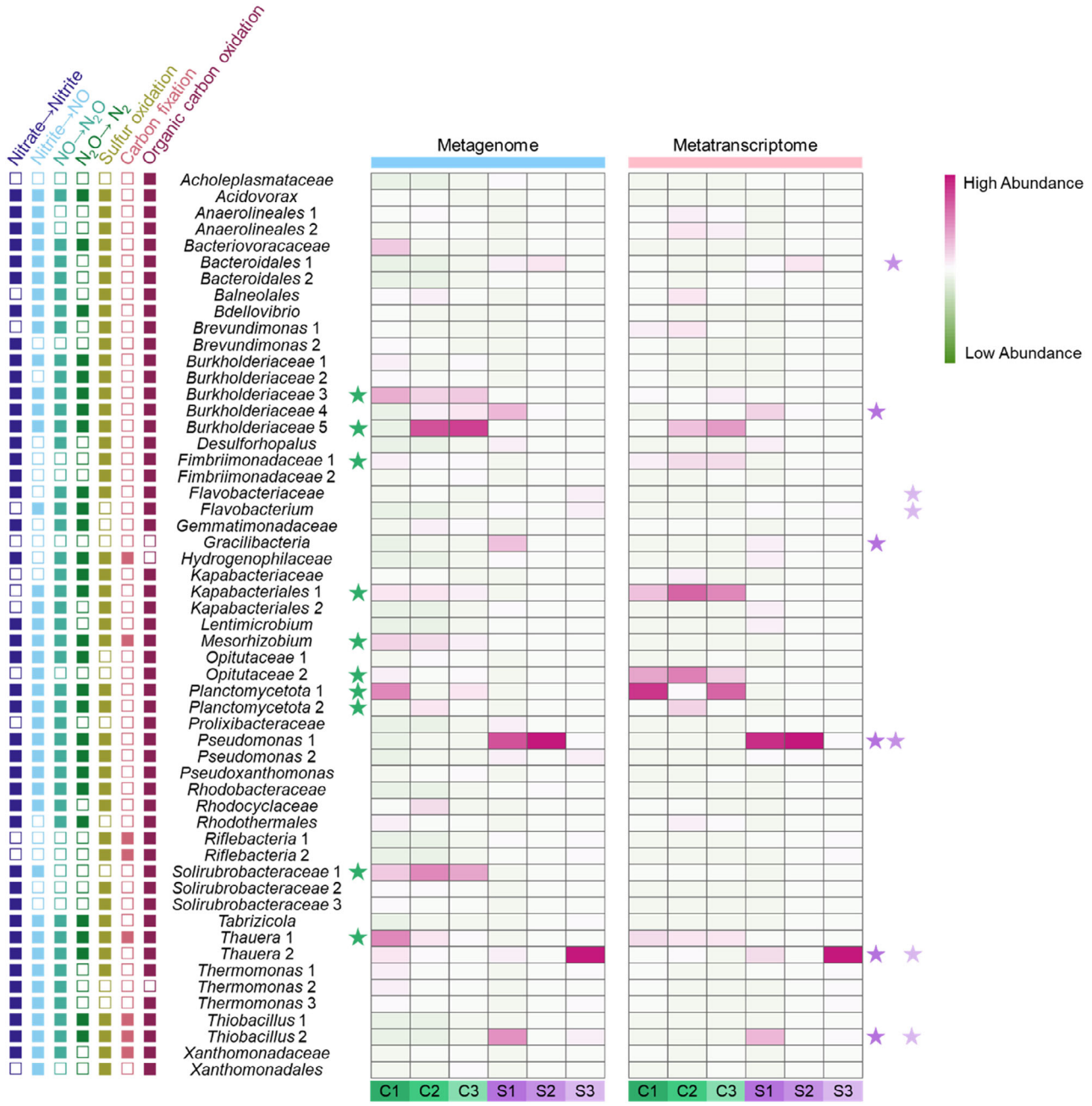

FIGURE 3 Functional potentials and relative abundance of populations associated with the recovered metagenome-assembled-genomes (MAGs) in both metagenomes and metatranscriptomes. Solid squares indicate the presence of the function and hollow squares indicate the absence of the function. The core populations in the systems with only acetate were indicated with stars in green on the left of the heatmap. The core populations in the systems with acetate and thiosulphate were different for the three replicates and indicated with stars in dark purple (S1), medium purple (S2), and light purple (S3) on the right of the heatmap.

presence of anammox-related enzyme encoding genes (i.e., the hydrazine synthase encoding gene *hzs* and the hydroxylamine dehydrogenase encoding gene *hzo*), while genes related to denitrification were especially abundant and highly transcribed. In metagenomes, the abundance of most genes involved in denitrification was over 50 times higher than the average abundance of all genes. In metatranscriptomes, periplasmic nitrate reductases encoded by *napA* and *napB* genes were more abundant in the systems without thiosulphate, while cytosolic nitrate reductases encoded by *narG* and *narH* genes were more abundant in the thiosulphate-based systems. For both treatments, the cytochrome cd1 heme type nitrite reductase encoded by *nirS* was more abundant than the copper-containing nitrite reductase encoded by *nirK*. For most samples, the transcript of nitric oxide reductase subunit encoding gene *norB* was over 400 times of average

14622920, 2023, 10, Downloaded from https://ami-journals.onlinelibrary.wiley.com/doi/10.1111/1462-2920.16430 by MPI 317 Marine Microbiology, Wiley Online Library on [22/01/2024]. See the Terms and Conditions (https://onlinelibrary.wiley.com/terms-and-conditions) on Wiley Online Library for rules of use; OA articles are governed by the applicable Creative Commons License

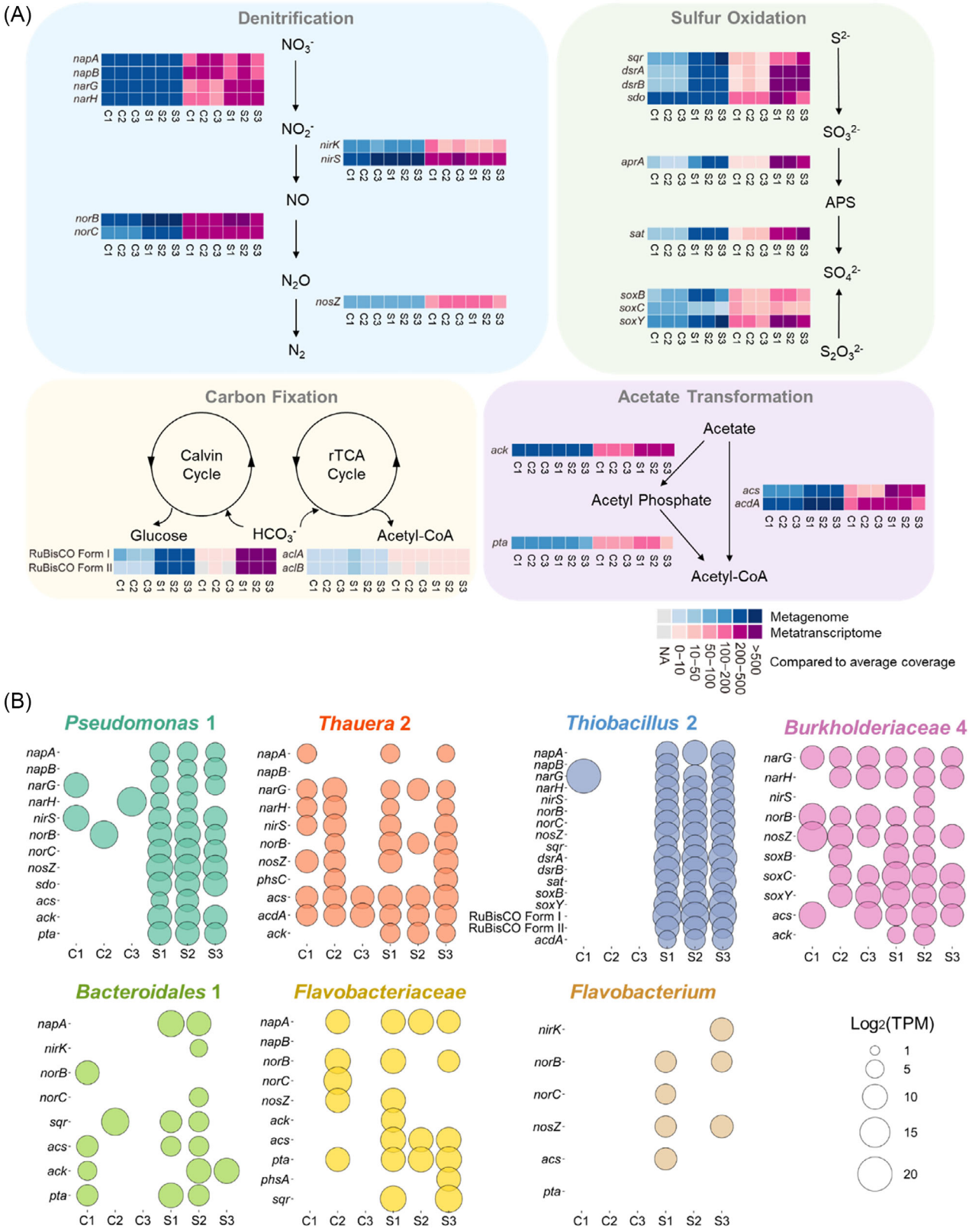

FIGURE 4 (A) Relative abundance of genes involved in denitrification, sulphur oxidation, carbon fixation, and acetate transformation in metagenomes and metatranscriptomes. The sequencing depth for each functional gene was normalized to the average sequencing depth of all genes. (B) Transcripts per million (TPM) of functional genes in the core populations (except *Gracilibacteria*) in the thiosulphate-based denitrifying systems. TPM calculation was based on each transcriptome affiliated with each population.

14622920, 2023, 10, Downloaded from https://ami-journals.onlinelibrary.wiley.com/doi/10.1111/1462-2920.16430 by MPI 317 Marine Microbiology, Wiley Online Library on [22/01/2024]. See the Terms and Conditions (https://onlinelibrary.wiley.com/terms-and-conditions) on Wiley Online Library for rules of use; OA articles are governed by the applicable Creative Commons License

transcription level and was even more highly transcribed in the thiosulphate-based systems. On the contrary, the abundance of nitrous oxide reductase *nosZ* was about 70 times of average abundance in metagenomes and about 100 times of average transcription level in metatranscriptomes. For sulphur oxidation, almost all related enzymes, including both the sulphide-quinone oxidoreductase (SQR) pathway and Sox (sulphur oxidation) system, were more actively expressed in the systems with thiosulphate than without thiosulphate (Figure 4A). For carbon fixation, the key enzymes of the Calvin Cycle, two main forms of RuBisCO, were more abundant with thiosulphate addition. The two pathways responsible for acetate transformation—first producing acetyl-CoA and then entering the tricarboxylic acid cycle (TCA cycle)—were also investigated. The pathway directly producing acetyl-CoA from acetate includes the use of AMP-forming acetyl-CoA synthetase (*acs*) or ADP-forming acetyl-CoA synthetase (*acdA*). Both of the synthetases were more abundant in the systems with thiosulphate. The other pathway first forms acetyl phosphate and then produces acetyl-CoA. The responsible enzymes, acetate kinase (*ack*) and phosphate acetyltransferase (*pta*) seemed to still be more actively transcribed in the systems with thiosulphate.

Transcription of the key enzymes of core populations in the thiosulphate-based systems was additionally investigated (Figure 4B). Here, TPM calculation was based on each population, which helped us identify highly expressed genes regardless of different population abundances in metatranscriptomes. For *Pseudomonas* 1 and *Thiobacillus* 2, genes involved in denitrification and sulphur oxidation were more actively transcribed in the systems with thiosulphate than in the systems without thiosulphate. Most core populations actively expressed enzyme-encoding genes involved in both sulphur and acetate utilization.

Transcriptomes of the enriched denitrifiers

Transcriptomes of a single population were analysed by mapping mRNA reads to each MAG. For the most abundant population in S1 and S2, *Pseudomonas* 1, the most highly expressed genes were involved in central dogma (DNA replication, transcription, and RNA translation), central metabolism, regulation, and respiration (Table S4). For example, thiosulphate dehydrogenase was highly expressed ($\log_2$(TPM) was 8.7 in S1 and 11.7 in S2), while nitrous oxide reductase was transcribed to a comparable level (11.8 in S1 and 11.4 in S2). Enzymes involved in central metabolism, including quinoprotein alcohol dehydrogenase (11.8 in S1 and 13.1 in S2), formate dehydrogenase-O major subunit (11.1 in S1 and 12.4 in S2), succinate dehydrogenase iron–sulphur subunit (11.7 in S1 and 10.4 in S2) and isocitrate dehydrogenase (10.4 in S1 and 10.2 in S2), also showed high transcriptional abundance. Some genes for regulation and defence were highly transcribed as well. Ribosome modulation factor *rmf* (16.3 in S1 and 15.8 in S2), ribosome hibernation promoting factor *hpf* (14.0 in S1 and 11.5 in S2), response regulator *pleD* (13.2 in S1 and 9.8 in S2) and catalase (14.3 in S1 and 10.0 in S2) for reactive oxygen species (ROS) defence all displayed above average gene expression levels. For the most abundant population in S3, *Thauera* 2 (Table S5), the 10 most abundant proteins included the cold shock protein CspE ($\log_2$(TPM) $= 16.1$ in S3), rubrerythrin (14.1) which was used for oxidative stress tolerance, iron–sulphur cluster insertion protein ErpA (13.7) which was essential for anaerobic respiration, cell division protein ZapA (13.5), 2-isopropylmalate synthase (13.5) for branched-chain amino acid biosynthetic process and ribosomal proteins (13.4).

The high expression of genes involved in central dogma, respiration, regulation, and defence was also detected in transcriptomes of other core organisms. For *Thiobacillus* 2 (Table S6), three enzymes for carbon fixation, ribulose bisphosphate carboxylase large chain ($\log_2$(TPM) was 13.6 in S1 and 12.1 in S3), small chain (13.6 in S1 and 10.3 in S3) and major carboxysome shell protein (13.9 in S1 and 7.7 in S3), were particularly actively expressed. Other examples for respiration, regulation, and defence were adenylylsulphate reductase subunit alpha (13.2 in S1 and 10.8 in S3) and beta (13.7 in S1 and 12.5 in S3), cold shock-like protein CspA (17.0 in S1 and 16.2 in S3) and rubrerythrin (14.0 in S1 and 12.6 in S3). For *Burkholderiaceae* 4 (Supplementary Table S7), the alkyl hydroperoxide reductase ($\log_2$(TPM) $= 14.6$ in S1) for ROS defence, chaperones, and ribosomal proteins were the most expressed proteins. More proteins for *Bacteroidales* 1 were annotated as hypothetical proteins (Table S8), but the active transcription of ribosomal proteins and proteins for defence, such as superoxide dismutase [Mn] ($\log_2$(TPM) $= 13.2$ in S2) and RNA polymerase factor (12.9), was still observed. For *Flavobacteriaceae* (Table S9), superoxide dismutase [Mn] ($\log_2$(TPM) $= 15.3$ in S3), cytochrome c551 (14.6), acyl carrier protein AcpP (14.4), cytochrome c6 (14.2), ATP-dependent Clp protease adapter protein ClpS (14.1), cold shock-like protein CspC (14.0) and thiol peroxidase (13.7) were the 10 most highly transcribed proteins. For *Flavobacterium* (Table S10), ribosomal proteins were most actively transcribed.

Microbial interactions between prototrophs and auxotrophs

The existence and expression of genes involved in the biosynthesis and transport of amino acids and vitamins

14622920, 2023, 10, Downloaded from https://ami-journals.onlinelibrary.wiley.com/doi/10.1111/1462-2920.16430 by MPI 317 Marine Microbiology, Wiley Online Library on [22/01/2024]. See the Terms and Conditions (https://onlinelibrary.wiley.com/terms-and-conditions) on Wiley Online Library for rules of use; OA articles are governed by the applicable Creative Commons License

in genomes of core populations were examined in each replicated thiosulphate-based system (Figure 5, Tables S13 and S14). As a disclaimer, this analysis was based on draft genomes which were not complete, so we only suggest the possibility of metabolic interactions in the systems. Several core populations were likely missing synthesis pathways of amino acids and vitamins. For example, the draft genome of *Thiobacillus* 2 did not have genes for the biosynthesis of aspartate, cysteine, phenylalanine, serine, threonine, tyrosine, cobalamin, and niacinamide. *Burkholderiaceae* 4 was likely not able to synthesize asparagine, aspartate, glutamine, histidine, folate, and pyridoxine. Even more essential genes for amino acid and vitamin synthesis were not present in the genomes of *Bacteroidales* 1, *Flavobacteriaceae*, and *Flavobacterium*, which were more complete and had less contamination (with the completeness of 97.3%, 95.1%, and 98.9%, respectively) (Table S1).

This was in contrast to the genomes of the two most abundant organisms—*Pseudomonas* 1 (completeness 91.6%) had genes for biosynthesis of all amino acids and vitamins, whereas *Thauera* 2 (completeness 89.2%) only lacked aspartate aminotransferase for aspartate synthesis. For aspartate, *Thauera* 2 might obtain it from *Flavobacterium* in S3. The transcriptome of *Pseudomonas* 1 did not contain enzymes for pyridoxine biosynthesis in S1, whereas we did not discover enzymes for serine biosynthesis in the transcriptome of *Thauera* 2 in S3. These two populations highly transcribed synthesis genes for most amino acids even including those with high bio-energy costs, such as tryptophan, phenylalanine, and tyrosine (Akashi & Gojobori, 2002). For example, 2-isopropylmalate synthase encoding gene *leuA* for leucine synthesis was highly expressed in the transcriptomes of both *Pseudomonas* 1 (log_2(TPM) was 11.4 in S1 and 11.8 in S2) and *Thauera* 2 (13.5 in S3) (Tables S4 and S5). Cysteine desulfurase IscS was also actively transcribed in *Pseudomonas* 1 (11.7 in S1 and 8.7 in S2) and *Thauera* 2 (10.3 in S3). In the transcriptome of *Thauera* 2, leucine/isoleucine/valine-binding protein (12.2), histidine biosynthesis bifunctional protein HisB (11.0), and cysteine desulfurase NifS (10.6) were highly expressed

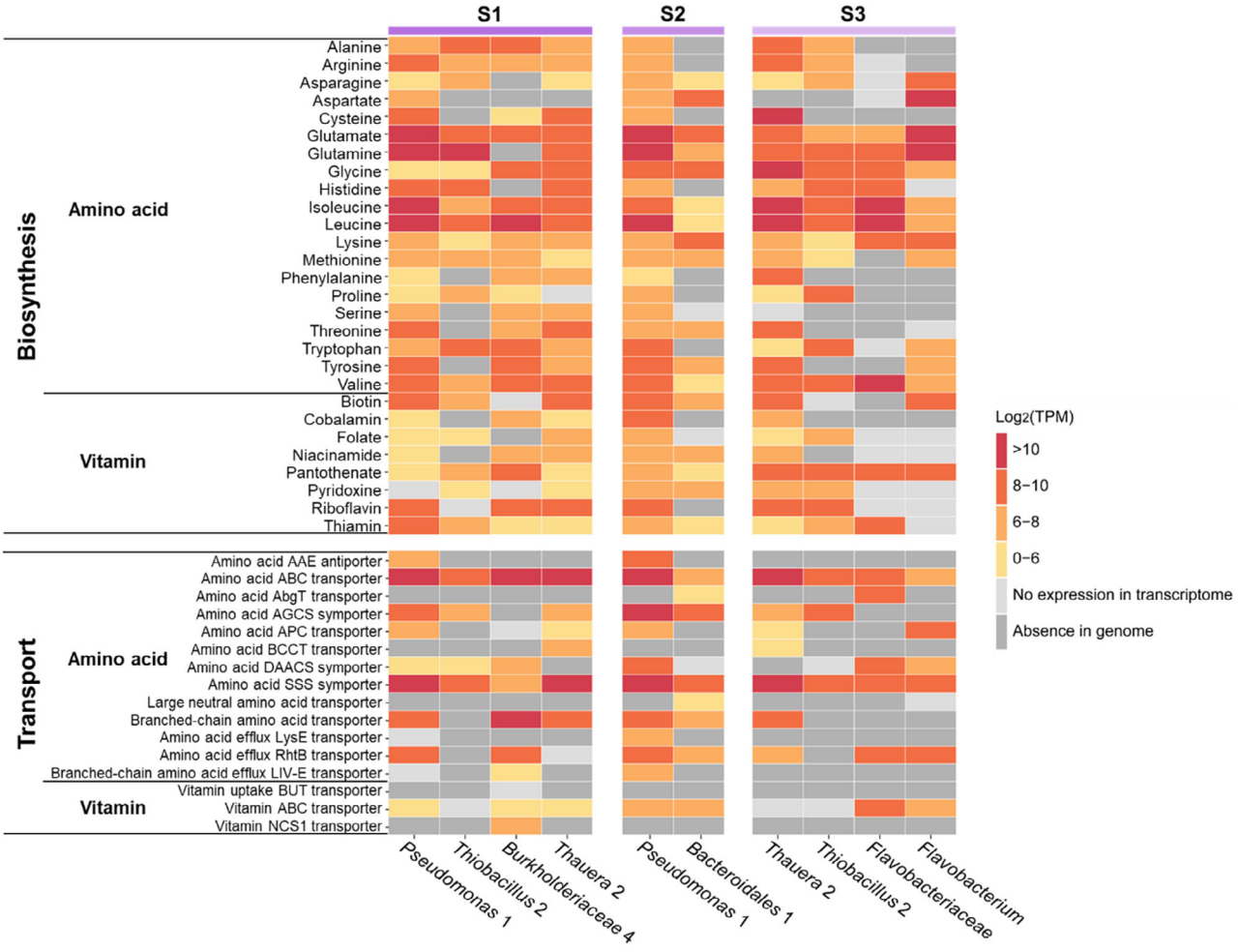

FIGURE 5 Relative expression of genes involved in biosynthesis and transport of amino acids and vitamins of core populations in the systems with thiosulphate.

14622920, 2023, 10, Downloaded from https://ami-journals.onlinelibrary.wiley.com/doi/10.1111/1462-2920.16430 by MPI 317 Marine Microbiology, Wiley Online Library on [22/01/2024]. See the Terms and Conditions (https://onlinelibrary.wiley.com/terms-and-conditions) on Wiley Online Library for rules of use; OA articles are governed by the applicable Creative Commons License

as well (Table S5). Genes encoding ABC-type transporters and SSS-type symporters with amino acids as substrates were highly expressed in almost all core populations (Figure 5, Table S13), facilitating the translocation of amino acids across membranes.

The genome of a previously isolated strain, *Pseudomonas* sp. C27, from a sulphur-dependent denitrifying system with an organic supplement, was analysed (Chen et al., 2013; Zhang et al., 2020). We found this genome only lacked the aspartate aminotransferase required for aspartate synthesis, whereas it contained all enzymes needed for vitamin biosynthesis, similar to the situations of *Pseudomonas* 1 and *Thauera* 2 recovered in this study. To check if prototrophy was a common characteristic for all *Pseudomonas* populations, the other *Pseudomonas* population in the system, *Pseudomonas* 2 (completeness 88.4%), was analysed (Table S12). The draft genome of *Pseudomonas* 2 lacked enzymes for the biosynthesis of asparagine, methionine, phenylalanine, cobalamin, and pyridoxine (Table S12). Though *Pseudomonas* 2 showed similar metabolisms to *Pseudomonas* 1, such as the complete denitrification capability, it was less abundant (less than 4% in the three replicates).

For core populations in the systems with only acetate, we did not observe a genome with the full set of genes needed for the synthesis of all amino acids and vitamins (Table S15). Even if the genome contained the related genes, it might not be expressed. For example, *Mesorhizobium* contained genes involved in the biosynthesis of most amino acids and vitamins, but only genes for glutamate, isoleucine, and valine synthesis were observed with transcriptomics.

DISCUSSION

Life strategies of core populations

In previously reported autotrophic denitrifying reactors with only reduced sulphur as the electron donor, species such as *Thiobacillus* and *Sulfurimonas* became dominant (Shao et al., 2010; Yang et al., 2016). However, in aquatic environments with the presence of organic compounds, the situation might be different. As suggested by the metagenome dataset, *Pseudomonas* and *Thauera* were the most abundant denitrifiers in the thiosulphate-based systems operated at low C/N ratio, with a few other populations together composing the core microbiome. The success of these populations might be explained by their life strategies and biotic interactions (Figure 6).

First, they adopted a heterotrophic lifestyle. According to previous studies, the commonly assumed autotrophic denitrifiers (e.g., *Thiobacillus* and *Sulfurimonas*) and heterotrophic denitrifiers (e.g., *Thauera* and *Acinetobacter*) jointly contributed to nitrate removal in sulphur-driven denitrifying systems supplemented with organic carbon (Han et al., 2020; Qiu et al., 2020; Zhang et al., 2018; Zhang et al., 2020). However, based on genome-centred metagenomics and metatranscriptomics, most core populations did not have genes responsible for carbon fixation in the genomes and they highly transcribed genes involved in sulphur oxidation, suggesting they were heterotrophic while using sulphur as the electron donor (Figure 4B). This survival strategy helped the cells enhance growth and gain an advantage in environments with low organic carbon content and extra inorganic electron donor supplied. A similar strategy was observed for cells encountering low organic substrate environments but with the presence of iron(II) (Chakraborty et al., 2011). This also answered the first research question of this study—the system led to the enrichment of a core microbiome that uses both organic compounds and the inorganic electron donor, instead of two functional groups. The previously considered two functional groups with distinct metabolisms were falsified by genome and transcriptome analysis.

In addition to respiration, high expression was observed for genes involved in central dogma, regulation, and defence in all core populations (Tables S4–S9). This indicated the cells were growing rapidly and promptly regulating their behaviour by regulators and defence proteins to obtain better growth and adapt well to the environments, which added to their success.

Metabolic interactions of core populations

Another aspect that increased the robustness of the core microbiome was related to microbial interactions. From the perspective of nitrogen metabolism, the most abundant populations in the three replicates of the thiosulphate-based systems were complete denitrifiers (Figures 3 and 4B). Mounting evidence showed that complete denitrifiers were the minority, with many microorganisms being specialists that perform only one or a few nitrogen oxide reduction reactions (Kuypers et al., 2018). Especially, the cooperation between nitrate to N_2O reducers and N_2O reducers to finish denitrification has been widely observed (Hallin et al., 2018; Jones et al., 2013). However, *Pseudomonas* 1 and *Thauera* 2 were independent in regards to nitrogen metabolism, not relying on others to finish denitrification, which could bring two benefits. First, the independence of denitrifiers avoids damage to nitrogen removal performance and community structure if a less abundant organism was impacted by some reason. Second, this might promote denitrification efficiency due to the reduction of the transport of nitrogen metabolites.

In addition, there was a robust syntrophic relationship among microorganisms through the nutritional

14622920, 2023, 10, Downloaded from https://ami-journals.onlinelibrary.wiley.com/doi/10.1111/1462-2920.16430 by MPI 317 Marine Microbiology, Wiley Online Library on [22/01/2024]. See the Terms and Conditions (https://onlinelibrary.wiley.com/terms-and-conditions) on Wiley Online Library for rules of use; OA articles are governed by the applicable Creative Commons License

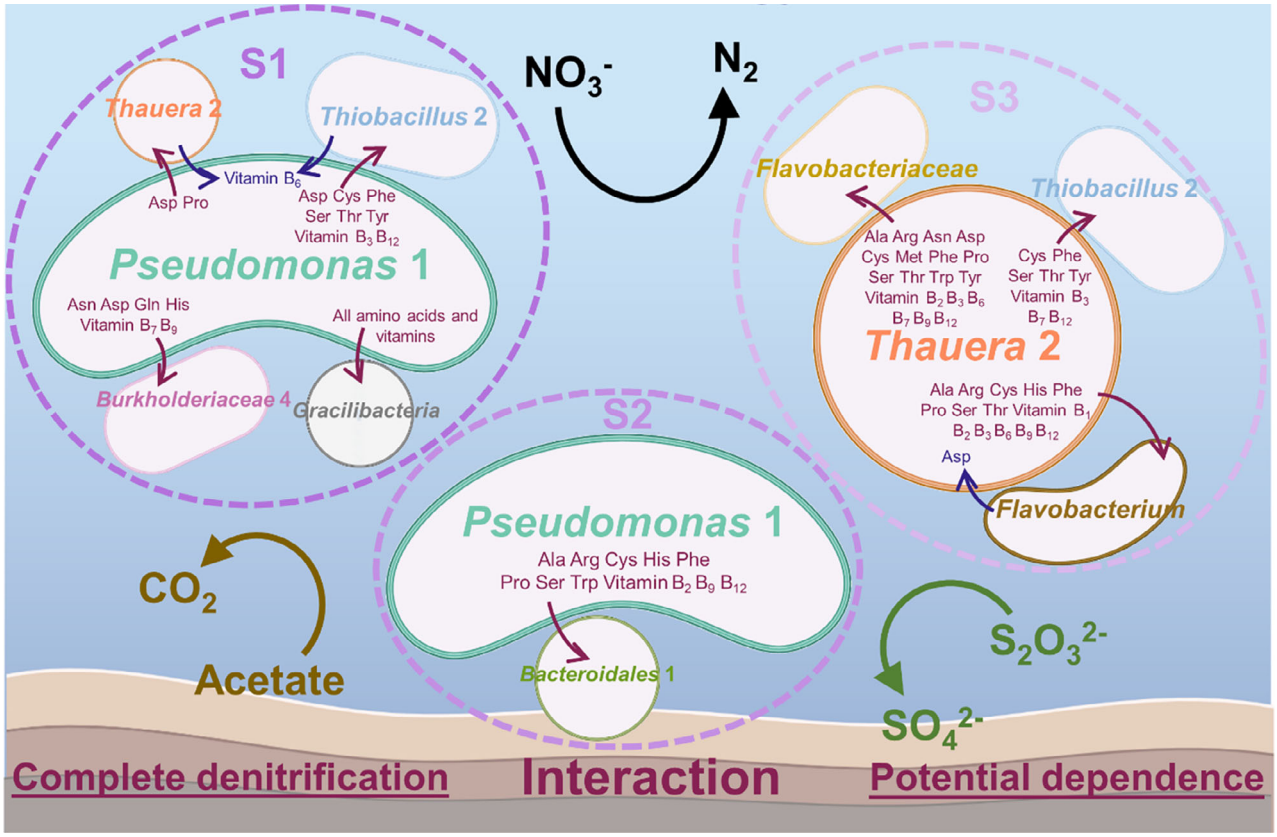

FIGURE 6 Proposed life strategies and metabolic interactions among core populations in the three replicates of the thiosulphate-based denitrifying systems.

requirement of amino acids and vitamins in the thiosulphate-based systems (Figure 5). Previous studies proposed that genomic loss of costly function and dependence among community members through the sharing of public goods were favoured at the individual level (Morris et al., 2012). Such dependence is a significant driver of community structure (Mas et al., 2016; Zengler & Zaramela, 2018). Particularly, the exchange of amino acids and vitamins among auxotrophic community members can greatly contribute to their composition (Zengler & Zaramela, 2018). For example, abundant denitrifiers were found to miss biosynthesis pathways for more amino acids and vitamins than other less abundant denitrifiers in a partial-nitritation anammox reactor (Wang et al., 2019). This might explain their abundance advantage, due to the reduction of metabolic burden. For another, cross-feedings of amino acids and vitamins were usually bidirectional (Embree et al., 2015; Liu et al., 2018; Wang et al., 2019), with some members providing specific substances and other members providing other required substances, forming intertwined dependencies.

However, the situation was different in the studied thiosulphate-based systems. We observed that the two most abundant populations, *Pseudomonas* 1 and *Thauera* 2, were able to synthesize almost all amino acids and vitamins. This was further confirmed with a previously discovered dominant organism isolated from a sulphide-based denitrifying system amended with acetate, *Pseudomonas* sp. C27, which could also synthesize almost all vitamins and amino acids (Chen et al., 2013; Zhang et al., 2020). Only aspartate was likely not self-supplied by *Thauera* 2 and *Pseudomonas* sp. C27, while aspartate is a low-cost amino acid and other community members were able to provide it. In contrast, less abundant core populations were likely to be auxotrophic. The other *Pseudomonas* population in the system, *Pseudomonas* 2, was also auxotrophic. Although *Pseudomonas* 2 showed similar abilities in carbon, sulphur, and nitrogen cycling pathways to *Pseudomonas* 1, it was much less abundant than *Pseudomonas* 1. Similar biochemical metabolisms but different nutritional biosynthesis might lead to their abundance difference. The requirement of auxotrophs for amino acids and vitamins was possibly satisfied by *Pseudomonas* 1 and *Thauera* 2, evidenced by the high expression of transport systems. Such a syntrophic relationship suggested that sulphur-based denitrifying systems might select for a prototrophic organism as the most abundant member. In this case, the most abundant members were 'helpers' and less abundant members were 'beneficiaries'. Mutual dependence reduces

14622920, 2023, 10, Downloaded from https://ami-journals.onlinelibrary.wiley.com/doi/10.1111/1462-2920.16430 by MPI 317 Marine Microbiology, Wiley Online Library on [22/01/2024]. See the Terms and Conditions (https://onlinelibrary.wiley.com/terms-and-conditions) on Wiley Online Library for rules of use; OA articles are governed by the applicable Creative Commons License

energy burden for single populations, but might also be deadly if one of the relationships was destructed. The relative independence enabled the survival of the most abundant organisms even when some of the other flanking members were destroyed. The flanking members could also survive only with the survival of the most abundant member, largely decreasing the risk of collapse of the whole community.

Implications of this study

The current study shed light on compositions, lifestyles, and metabolic interactions of the core microbiome in the thiosulphate-based denitrifying system. Microbial community compositions were not the same in the three replicates. Similar things were observed in a previous study—different communities were assembled with the same inoculation under identical environmental conditions (Zhou et al., 2013). However, the three replicates showed similar denitrification performance after an adaptation period (the first and second phases) (Figure 1B). This observation supported the 'function over phylogeny' theory—environmental conditions select for similar functional community structures despite highly variable taxonomic compositions (Gibbons, 2017; Louca et al., 2016). In the thiosulphate-based denitrifying system, functions for carbon, nitrogen, and sulphur cycling processes were similar (Figure 4A), but microbial taxa were enriched to different extents (Figure 3). The variance among replicates could result from biotic interactions, ecological drift, and dispersal limitation (Zhou & Ning, 2017). As drift and dispersal are hard to discern in laboratory-modelled systems, we mainly analysed biotic interactions. The findings revealed that the energy burden for the biosynthesis of amino acids and vitamins was not distributed evenly among core populations. Even if different species were enriched, the most abundant organism was always the most stressed one. Some studies showed the importance of rare organisms in producing common goods and thus preserving community stability (Konopka et al., 2015), but our findings highlighted less abundant members depended on the most abundant organism. Furthermore, the most abundant organism was also a complete denitrifier, without a need to rely on others to consume or provide intermediate metabolites during denitrification. The relative independence of the most abundant members and relative dependence of less abundant members might shape microbial community assembly.

The most abundant organisms were also likely dominant organisms participating in nitrate removal. Nutrition biosynthesis is energy-intensive, thus, seeking a way to reduce the burden of biosynthesis of the dominant organisms might greatly improve nitrogen removal performance. For example, externally adding amino acids and vitamins, especially those with less flanking populations able to synthesize (e.g., aspartate, phenylalanine, and cobalamin), to the system might enable the most abundant member to focus metabolism more on denitrification, further facilitating nitrate removal. Our study was mainly based on genome and transcriptome analysis. Future studies could further investigate the availability of amino acids and vitamins in free medium and their amenability for exchange among microbial populations with advanced approaches such as NanoSIMS or by building a synthetic microbial community. Future studies could also evaluate the benefits of nutrition supplementation on nitrogen removal during sulphur-based denitrification for engineering purposes.

CONCLUSIONS

A thiosulphate-based denitrifying system was established and performed well in nitrate removal compared to the system with only acetate supplied. Genome-centred metagenomics and metatranscriptomics revealed microbial populations and potential metabolic interactions in the thiosulphate-based denitrifying consortium. All of the core populations used sulphur as the electron donor. They actively expressed genes for denitrification, sulphur oxidation, and acetate transformation. Although different enrichments were observed for the three replicates, the most abundant members in the systems were complete denitrifiers. Furthermore, the most abundant populations were relatively prototrophic, able to synthesize almost all amino acids and vitamins and supply the substances to flanking community members. The findings added new and fundamental insights into the microbial world for thiosulphate-based denitrification, with implications for the environmental remediation of nitrate-polluted water bodies.

AUTHOR CONTRIBUTIONS

Shengjie Li: Conceptualization (equal); formal analysis (lead); investigation (lead); methodology (lead); visualization (lead); writing – original draft (lead); writing – review and editing (equal). **Yinhao Liao:** Investigation (supporting); methodology (supporting). **Zhuo Jiang:** Investigation (supporting). **Guodong Ji:** Conceptualization (equal); funding acquisition (lead); project administration (lead); supervision (lead); writing – review and editing (equal).

ACKNOWLEDGEMENTS

This research was supported by the Foundation for Innovative Research Groups of the National Natural Science Foundation of China (No. 51721006) and the National Key Research and Development Project of China (No. 2019YFC0409200). Sequence analysis was supported by the High-performance Computing Platform of Peking University.

14622920, 2023, 10, Downloaded from https://ami-journals.onlinelibrary.wiley.com/doi/10.1111/1462-2920.16430 by MPI 317 Marine Microbiology, Wiley Online Library on [22/01/2024]. See the Terms and Conditions (https://onlinelibrary.wiley.com/terms-and-conditions) on Wiley Online Library for rules of use; OA articles are governed by the applicable Creative Commons License

CONFLICT OF INTEREST STATEMENT

The authors declare no conflict of interest.

DATA AVAILABILITY STATEMENT

All sequences of this study are available at NCBI (PRJNA848245). The Biosamples for the 16S rRNA sequences are SAMN28990699–SAMN28990740. The Biosamples for the MAGs are SAMN28990796–SAMN28990850. The Biosamples for the metagenome raw reads are SAMN28990744–SAMN28990749. The Biosamples for the metatranscriptome reads are SAMN28990753–SAMN28990758.

ORCID

Guodong Ji https://orcid.org/0000-0002-0195-2367

REFERENCES

Akashi, H. & Gojobori, T. (2002) Metabolic efficiency and amino acid composition in the proteomes of Escherichia coli and Bacillus subtilis. *Proceedings of the National Academy of Sciences of the United States of America*, 99(6), 3695–3700.

Anders, S., Pyl, P.T. & Huber, W. (2015) HTSeq—a python framework to work with high-throughput sequencing data. *Bioinformatics*, 31(2), 166–169.

Callahan, B.J., McMurdie, P.J., Rosen, M.J., Han, A.W., Johnson, A. J. & Holmes, S.P. (2016) DADA2: high-resolution sample inference from Illumina amplicon data. *Nature Methods*, 13(7), 581–583.

Chakraborty, A., Roden, E.E., Schieber, J. & Picardal, F. (2011) Enhanced growth of Acidovorax sp. strain 2AN during nitrate-dependent Fe(II) oxidation in batch and continuous-flow systems. *Applied and Environmental Microbiology*, 77(24), 8548–8556.

Chen, C., Ho, K.L., Liu, F.C., Ho, M., Wang, A., Ren, N. et al. (2013) Autotrophic and heterotrophic denitrification by a newly isolated strain *Pseudomonas* sp. C27. *Bioresource Technology*, 145, 351–356.

Chen, S., Zhou, Y., Chen, Y. & Gu, J. (2018) Fastp: an ultra-fast all-in-one FASTQ preprocessor. *Bioinformatics*, 34(17), i884–i890.

Della Rocca, C., Belgiorno, V. & Meriç, S. (2007) Overview of in-situ applicable nitrate removal processes. *Desalination*, 204(1–3), 46–62.

Eddy, S.R. (2008) A probabilistic model of local sequence alignment that simplifies statistical significance estimation. *PLoS Computational Biology*, 4(5), e1000069.

Embree, M., Liu, J.K., Al-Bassam, M.M. & Zengler, K. (2015) Networks of energetic and metabolic interactions define dynamics in microbial communities. *Proceedings of the National Academy of Sciences of the United States of America*, 112(50), 15450–15455.

Faust, K. & Raes, J. (2012) Microbial interactions: from networks to models. *Nature Reviews Microbiology*, 10(8), 538–550.

Gibbons, S.M. (2017) Microbial community ecology: function over phylogeny. *Nature Ecology and Evolution*, 1(1), 32.

Hallin, S., Philippot, L., Loffler, F.E., Sanford, R.A. & Jones, C.M. (2018) Genomics and ecology of novel N2O-reducing microorganisms. *Trends in Microbiology*, 26(1), 43–55.

Han, F., Zhang, M., Shang, H., Liu, Z. & Zhou, W. (2020) Microbial community succession, species interactions and metabolic pathways of sulfur-based autotrophic denitrification system in organic-limited nitrate wastewater. *Bioresource Technology*, 315, 123826.

Haroon, M.F., Hu, S., Shi, Y., Imelfort, M., Keller, J., Hugenholtz, P. et al. (2013) Anaerobic oxidation of methane coupled to nitrate reduction in a novel archaeal lineage. *Nature*, 500(7464), 567–570.

He, S., Tominski, C., Kappler, A., Behrens, S. & Roden, E.E. (2016) Metagenomic analyses of the autotrophic Fe(II)-oxidizing, nitrate-reducing enrichment culture KS. *Applied and Environmental Microbiology*, 82(9), 2656–2668.

Jones, C.M., Graf, D.R., Bru, D., Philippot, L. & Hallin, S. (2013) The unaccounted yet abundant nitrous oxide-reducing microbial community: a potential nitrous oxide sink. *The ISME Journal*, 7(2), 417–426.

Kang, D.D., Li, F., Kirton, E., Thomas, A., Egan, R., An, H. et al. (2019) MetaBAT 2: an adaptive binning algorithm for robust and efficient genome reconstruction from metagenome assemblies. *PeerJ*, 7, e7359.

Konopka, A., Lindemann, S. & Fredrickson, J. (2015) Dynamics in microbial communities: unraveling mechanisms to identify principles. *The ISME Journal*, 9(7), 1488–1495.

Kopylova, E., Noe, L. & Touzet, H. (2012) SortMeRNA: fast and accurate filtering of ribosomal RNAs in metatranscriptomic data. *Bioinformatics*, 28(24), 3211–3217.

Kuypers, M.M.M., Marchant, H.K. & Kartal, B. (2018) The microbial nitrogen-cycling network. *Nature Reviews Microbiology*, 16(5), 263–276.

Li, D., Liu, C.M., Luo, R., Sadakane, K. & Lam, T.W. (2015) MEGAHIT: an ultra-fast single-node solution for large and complex metagenomics assembly via succinct de Bruijn graph. *Bioinformatics*, 31(10), 1674–1676.

Li, R., Feng, C., Hu, W., Xi, B., Chen, N., Zhao, B. et al. (2016) Woodchip-sulfur based heterotrophic and autotrophic denitrification (WSHAD) process for nitrate contaminated water remediation. *Water Research*, 89, 171–179.

Li, R., Feng, C., Xi, B., Chen, N., Jiang, Y., Zhao, Y. et al. (2017) Nitrate removal efficiency of a mixotrophic denitrification wall for nitrate-polluted groundwater in situ remediation. *Ecological Engineering*, 106, 523–531.

Li, S., Jiang, Z. & Ji, G. (2022a) Effect of sulfur sources on the competition between denitrification and DNRA. *Environmental Pollution*, 305, 119322.

Li, S., Liao, Y., Pang, Y., Dong, X., Strous, M. & Ji, G. (2022b) Denitrification and dissimilatory nitrate reduction to ammonia in long-term lake sediment microcosms with iron(II). *Science of the Total Environment*, 807(1), 150835.

Li, S., Luo, Z. & Ji, G. (2018) Seasonal function succession and biogeographic zonation of assimilatory and dissimilatory nitrate-reducing bacterioplankton. *Science of the Total Environment*, 637-638, 1518–1525.

Li, S., Mosier, D., Dong, X., Kouris, A., Ji, G., Strous, M. and Diao, M. (2022c) Frequency of change determines effectiveness of microbial response strategies in sulfidic stream microbiomes. bioRxiv

Li, S., Pang, Y. & Ji, G. (2021) Increase of N2O production during nitrate reduction after long-term sulfide addition in lake sediment microcosms. *Environmental Pollution*, 291, 118231.

Li, W. & Godzik, A. (2006) Cd-hit: a fast program for clustering and comparing large sets of protein or nucleotide sequences. *Bioinformatics*, 22(13), 1658–1659.

Liu, Y.F., Galzerani, D.D., Mbadinga, S.M., Zaramela, L.S., Gu, J.D., Mu, B.Z. et al. (2018) Metabolic capability and in situ activity of microorganisms in an oil reservoir. *Microbiome*, 6(1), 5.

Louca, S., Jacques, S.M.S., Pires, A.P.F., Leal, J.S., Srivastava, D. S., Parfrey, L.W. et al. (2016) High taxonomic variability despite stable functional structure across microbial communities. *Nature Ecology and Evolution*, 1(1), 15.

Magoc, T. & Salzberg, S.L. (2011) FLASH: fast length adjustment of short reads to improve genome assemblies. *Bioinformatics*, 27(21), 2957–2963.

Mas, A., Jamshidi, S., Lagadeuc, Y., Eveillard, D. & Vandenkoornhuyse, P. (2016) Beyond the black queen hypothesis. *The ISME Journal*, 10(9), 2085–2091.

McCullough, H. (1967) The determination of ammonia in whole blood by a direct colorimetric method. *Clinica Chimica Acta*, 17(2), 297–304.

14622920, 2023, 10, Downloaded from https://ami-journals.onlinelibrary.wiley.com/doi/10.1111/1462-2920.16430 by MPI 317 Marine Microbiology, Wiley Online Library on [22/01/2024]. See the Terms and Conditions (https://onlinelibrary.wiley.com/terms-and-conditions) on Wiley Online Library for rules of use; OA articles are governed by the applicable Creative Commons License

Mekonnen, M.M. & Hoekstra, A.Y. (2015) Global gray water footprint and water pollution levels related to anthropogenic nitrogen loads to fresh water. *Environmental Science and Technology*, 49(21), 12860–12868.

Morris, J.J., Lenski, R.E. & Zinser, E.R. (2012) The black queen hypothesis: evolution of dependencies through adaptive gene loss. *MBio*, 3(2), e00036–e00012.

Newcomer, T.A., Kaushal, S.S., Mayer, P.M., Shields, A.R., Canuel, E.A., Groffman, P.M. et al. (2012) Influence of natural and novel organic carbon sources on denitrification in forest, degraded urban, and restored streams. *Ecological Monographs*, 82(4), 449–466.

Olm, M.R., Brown, C.T., Brooks, B. & Banfield, J.F. (2017) dRep: a tool for fast and accurate genomic comparisons that enables improved genome recovery from metagenomes through de-replication. *The ISME Journal*, 11(12), 2864–2868.

Parks, D.H., Chuvochina, M., Waite, D.W., Rinke, C., Skarshewski, A., Chaumeil, P.A. et al. (2018) A standardized bacterial taxonomy based on genome phylogeny substantially revises the tree of life. *Nature Biotechnology*, 36(10), 996–1004.

Parks, D.H., Imelfort, M., Skennerton, C.T., Hugenholtz, P. & Tyson, G.W. (2015) CheckM: assessing the quality of microbial genomes recovered from isolates, single cells, and metagenomes. *Genome Research*, 25(7), 1043–1055.

Qiu, Y.Y., Zhang, L., Mu, X., Li, G., Guan, X., Hong, J. et al. (2020) Overlooked pathways of denitrification in a sulfur-based denitrification system with organic supplementation. *Water Research*, 169, 115084.

Seemann, T. (2014) Prokka: rapid prokaryotic genome annotation. *Bioinformatics*, 30(14), 2068–2069.

Seitzinger, S. (2008) Nitrogen cycle: out of reach. *Nature*, 452(7184), 162–163.

Shao, M.F., Zhang, T. & Fang, H.H. (2010) Sulfur-driven autotrophic denitrification: diversity, biochemistry, and engineering applications. *Applied Microbiology and Biotechnology*, 88(5), 1027–1042.

Wang, Y., Niu, Q., Zhang, X., Liu, L., Wang, Y., Chen, Y. et al. (2019) Exploring the effects of operational mode and microbial interactions on bacterial community assembly in a one-stage partial-nitritation anammox reactor using integrated multi-omics. *Microbiome*, 7(1), 122.

Yang, W., Lu, H., Khanal, S.K., Zhao, Q., Meng, L. & Chen, G.H. (2016) Granulation of sulfur-oxidizing bacteria for autotrophic denitrification. *Water Research*, 104, 507–519.

Zengler, K. & Zaramela, L.S. (2018) The social network of microorganisms - how auxotrophies shape complex communities. *Nature Reviews Microbiology*, 16(6), 383–390.

Zhang, L., Zhang, C., Hu, C., Liu, H., Bai, Y. & Qu, J. (2015) Sulfur-based mixotrophic denitrification corresponding to different electron donors and microbial profiling in anoxic fluidized-bed membrane bioreactors. *Water Research*, 85, 422–431.

Zhang, R.-C., Chen, C., Shao, B., Wang, W., Xu, X.-J., Zhou, X. et al. (2020) Heterotrophic sulfide-oxidizing nitrate-reducing bacteria enables the high performance of integrated autotrophic-heterotrophic denitrification (IAHD) process under high sulfide loading. *Water Research*, 178, 115848.

Zhang, R.C., Xu, X.J., Chen, C., Xing, D.F., Shao, B., Liu, W.Z. et al. (2018) Interactions of functional bacteria and their contributions to the performance in integrated autotrophic and heterotrophic denitrification. *Water Research*, 143, 355–366.

Zhou, J., Liu, W., Deng, Y., Jiang, Y.H., Xue, K., He, Z. et al. (2013) Stochastic assembly leads to alternative communities with distinct functions in a bioreactor microbial community. *MBio*, 4(2), e00584–e00512.

Zhou, J. & Ning, D. (2017) Stochastic community assembly: does it matter in microbial ecology? *Microbiology and Molecular Biology Reviews*, 81(4), e00002–e00017.

Zhou, W., Liu, X., Dong, X., Wang, Z., Yuan, Y., Wang, H. et al. (2016) Sulfur-based autotrophic denitrification from the micro-polluted water. *Journal of Environmental Sciences*, 44, 180–188.

Zhou, Z., Tran, P.Q., Breister, A.M., Liu, Y., Kieft, K., Cowley, E.S. et al. (2022) METABOLIC: high-throughput profiling of microbial genomes for functional traits, metabolism, biogeochemistry, and community-scale functional networks. *Microbiome*, 10(1), 33.

SUPPORTING INFORMATION

Additional supporting information can be found online in the Supporting Information section at the end of this article.

How to cite this article: Li, S., Liao, Y., Jiang, Z. & Ji, G. (2023) Life strategies and metabolic interactions of core microbes during thiosulphate-based denitrification. *Environmental Microbiology*, 25(10), 1925–1939. Available from: https://doi.org/10.1111/1462-2920.16430

14622920, 2023, 10, Downloaded from https://ami-journals.onlinelibrary.wiley.com/doi/10.1111/1462-2920.16430 by MPI 317 Marine Microbiology, Wiley Online Library on [22/01/2024]. See the Terms and Conditions (https://onlinelibrary.wiley.com/terms-and-conditions) on Wiley Online Library for rules of use; OA articles are governed by the applicable Creative Commons License